Resonant terahertz generation from InN thin films

Xiaodong Mu,[1] Yujie J. Ding,[1,*] Kejia Wang,[2] Debdeep Jena,[2] and Yuliya B. Zotova[3]

[1]*Department of Electrical and Computer Engineering, Lehigh University, Bethlehem, Pennsylvania 18015, USA*
[2]*Department of Electrical Engineering, University of Notre Dame, Notre Dame, Indiana 46556, USA*
[3]*ArkLight, P.O. Box 2, Center Valley, Pennsylvania 18034, USA*
**Corresponding author: yud2@lehigh.edu*

Received January 19, 2007; revised February 8, 2007; accepted March 4, 2007;
posted March 12, 2007 (Doc. ID 79234); published April 30, 2007

Highly efficient conversion from ultrafast optical pulses to their terahertz (THz) counterparts has been achieved with InN thin films. An average THz output power as high as 0.931 μW has been obtained for an average pump power of 1 W, corresponding to a normalized conversion efficiency of 190% mm^{-2}. Based on our measured dependences of the THz output power on pump polarization, incident angle, pump power, and InN film thickness, resonance-enhanced optical rectification is one of the most plausible mechanisms for the THz generation in the InN films. © 2007 Optical Society of America

OCIS codes: 190.2620, 190.7110, 320.7110.

ZnTe and InAs crystals remain the most efficient inorganic semiconductor electro-optic materials for terahertz (THz) generation by using ultrafast laser pulses. Optical rectification [1] and photo-Dember effect [2] are the primary mechanisms for THz generation in these two materials. Recently, InN films were used for generating THz radiation by using ultrafast laser pulses [3,4]. The mechanism for the THz generation was assigned to either the transient photocurrent [3] or the photo-Dember effect [4].

In this Letter, we present our results on efficient THz generation from InN thin films by using ultrafast laser pulses. A Ti:sapphire regenerative amplifier with the output wavelength, pulse width, and repetition rate of 790 nm, 180 fs, and 250 kHz, respectively, was used as a pump. After passing through a half-wave plate, the amplifier beam was focused by a positive lens ($f \approx 50$ mm). Each InN sample was sequentially placed in the beam path with the InN side being illuminated by the incoming beam at a location 5 mm from the focal point either before or after it (the beam diameter is 400 μm); see the inset of Fig. 1(a). The THz beam generated in the forward direction was then collected by a parabolic mirror and subsequently detected by an accurately calibrated bolometer. Polyethylene and germanium filters were inserted in front of the bolometer to block the unconverted pump beam.

Nine InN films were grown on (0001) sapphire substrates, each of which had a 4 μm semi-insulating GaN buffer layer grown by a Vecco Gen 930 molecular-beam epitaxy system at 490°–510°C; see Table 1. X-ray diffraction studies confirmed that these InN films all had a wurtzite structure with their *c* axis perpendicular to the substrate surface [5]. Although these InN films were not intentionally doped, they all had quite high electron densities; see Table 1. The bandgaps of these films were measured by us to be about 0.6 eV. For each InN film sample, we measured the THz output powers at different pump powers. Among all the samples, the highest output power achieved in our experiment was 0.931 μW for an average pump power of 1 W from the 700 nm thick InN film, i.e., sample 3 in Table 1. Moreover, the THz powers from all the InN films were independent of the azimuth angle, similar to Ref. [3]. However, the THz output power strongly de-

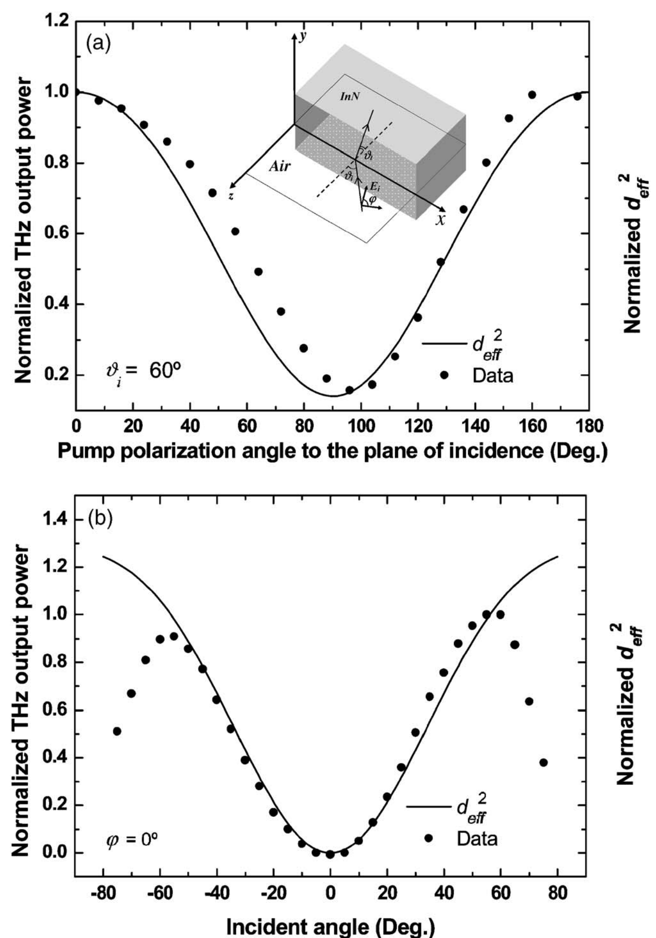

Fig. 1. Normalized output power (dots) and square of the effective nonlinear coefficient (solid curves) plotted as a function of (a) polarization angle for the pump beam and (b) incident angle of the pump beam. All the results were obtained on sample 3 at a pump power of 1 W. Inset, configuration for THz generation from an InN film.

0146-9592/07/111423-3/$15.00 © 2007 Optical Society of America

Table 1. Description of InN Samples Investigated in Our Experiment

Sample No.	InN Thickness (mm)	Mobility at 300 K $[cm^2/(V\,s)]$	Electron Density $(\times 10^{14}\ cm^{-2})$	Highest THz Output (nW)
1	1270	870	6.2	124
2	740	1054	3.02	576
3	700	735.8	2.52	931
4	600	593	6.1	175
5	300	534	3.93	192
6	150	278.5	3.28	60
7	70	—	—	15
8	50	—	—	5.8
9	25	—	—	0.5

pended on the polarization and incident angle of the pump beam; see Figs. 1(a) and 1(b). The maximum output power occurred at $\theta_i \approx 60°$ and for a p-polarized pump beam (i.e., $\varphi \approx 0°$, where φ is the angle of the pump polarization formed with respect to the plane of incidence); see the inset in Fig. 1(a). In such a case, the THz beam was measured as p-polarized by using a wire-grid polarizer. When the pump polarization was s polarized (i.e., $\varphi \approx 90°$), the output power was dramatically reduced from the maximum value. The ratio between the maximum and the minimum output powers was determined to be 6.4. Such a large ratio cannot be induced by the polarization dependence of the overlap between the photocarrier distribution and high-electric-field region observed in [6]. In our experiment, we used a much larger beam diameter, much thinner samples, and an incident angle of 60°.

The output power quadratically depended on the pump power when the pump power was less than 80 mW; see Fig. 2. For higher pump powers, however, the dependence approached linear. Since the photon energy of the pump beam was above the bandgap of the InN films, the absorption of the pump beam by the film could be quite high [7]. Therefore, at relatively higher pump powers the temperature of the film within the pumping area was significantly increased, which might have caused the absorption coefficient to increase [8]. One can see from Fig. 3 that the THz output powers from samples 3 and 5–8 form a quadratic dependence on the film thickness. However, for samples 1 and 4 the output powers were much less than those from sample 3, probably because of the much higher free-carrier absorption losses for the THz beams.

Among all the possible mechanisms for the THz generation, optical rectification is one of the most plausible. It can be readily shown [9] that although the second-order nonlinear polarization for our experimental configuration is independent of the azimuth angle, it strongly depends on the incident angle and the polarization of the pump beam. Furthermore, the square of the effective nonlinear coefficient is given by $d_{\mathrm{eff}}^2 = (d_x \cos\theta_t + d_z \sin\theta_t)^2 + d_y^2$, where d_x, d_y, and d_z are

$$d_x = 2d_{31}\cos^2\varphi\cos\theta_t\sin\theta_t$$

$$d_y = 2d_{31}\cos\varphi\sin\varphi\sin\theta_t$$

$$d_z = d_{31}\cos^2\varphi\cos^2\theta_t + d_{31}\sin^2\varphi + d_{33}\cos^2\varphi\sin^2\theta_t. \quad (1)$$

In Eq. (1) θ_t is the incident angle for the pump beam inside the InN film, and the x and y axes are chosen to be parallel to and perpendicular to the plane of incidence, respectively. In Fig. 1(a), d_{eff}^2 is plotted versus φ for $\theta_i = 60°$ by assuming that $d_{31} = d_{15}$ and $d_{33} = -2d_{15}$ [10]. Although the first relation is valid for a lossless medium [9], we can still use it as an approximation. The second one is derived from bond additivity [11]. Under these assumptions, d_{eff}^2 closely matches our data; see Fig. 1(a). Similarly, the dependence of d_{eff}^2 on θ_i for $\varphi = 0°$ is in excellent agreement with our data for $\theta_i < 60°$; see Fig. 1(b). Above 60°, however, the measured output power starts to decrease, probably because of the reflection losses for the two interacting beams. At the pump power of 1 W the output power is still proportional to the square of the effective nonlinear coefficient; see below. Although it was demonstrated previously that THz generation due to the transient photocurrent was efficient for the p-polarized pump [12], the calculated ratio between the maximum and the minimum output powers based on such a mechanism is much less than our experimental value. Furthermore, if $\theta_i \approx 60°$ corresponds to the Brewster angle for the pump beam, the index of refraction would be too small [13]. For normal incidence ($\theta = 0°$) the output power was measured by us to be close to zero. Although we tried to collect any THz beam that might have propagated in a direction forming an angle with that of the pump

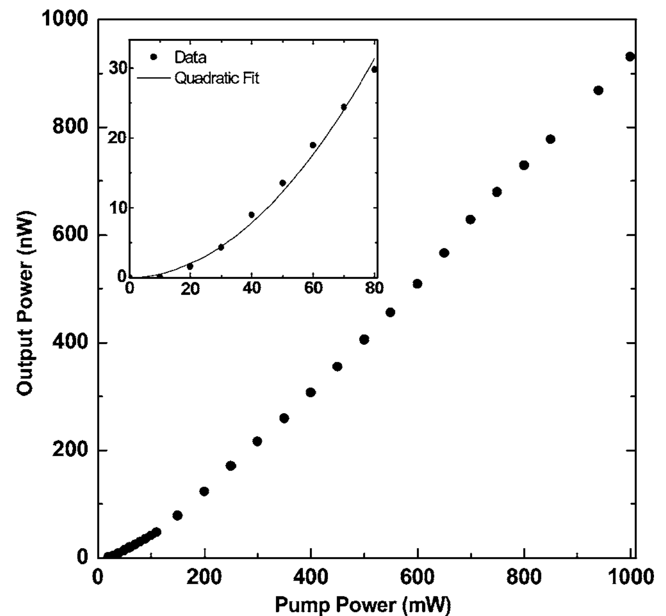

Fig. 2. Average output power plotted as a function of average pump power, measured on sample 3 (dots). The solid curve in the inset corresponds to the quadratic least-squares fit to our experimental results.

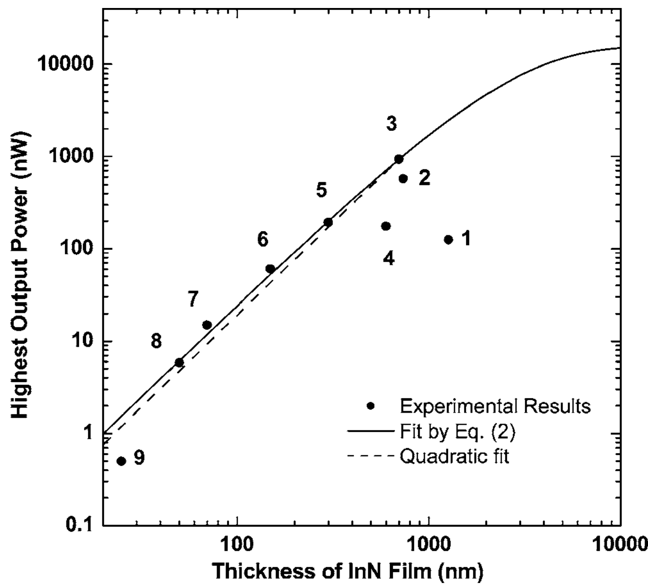

Fig. 3. Highest average output power for the THz radiation plotted as a function of InN film thickness, measured by us (dots). Dashed curve, fitting based on a quadratic dependence; solid curve, nonlinear least-squares fit to our data after the absorption for the pump beam is taken into consideration.

beam, the total output power was not measurable. Based on these characteristics, we have ruled out the transient photocurrent.

Based on optical rectification [14], the average output power is shown to be

$$P_{T,a} \approx \frac{0.6038\,\eta_0 d_{\text{eff}}^2 P_{p,a} P_p [1-\exp(-\alpha L)]^2}{c^2 n_{pg} n_p^2 \tau_p^2 a_p \alpha^2}, \qquad (2)$$

where τ_p is the pulse width, n_p and n_{pg} are the phase and group indices, p_p and $p_{p,a}$ are the peak and average powers, and α is the absorption coefficient, all for the pump beam; η_0 is the vacuum impedance; and L is the thickness of the film. One can see from Eq. (2) that the output power quadratically depends on the thickness of the film, which is consistent with our experimental results; see Fig. 3. Since the photon energy at the pump wavelength is well above the bandgap of the InN films, the absorption of the pump beam can be large, especially for thick films. Using α as an adjustable parameter, we have achieved the nonlinear least-squares fitting of our data by using Eq. (2) when $\alpha \approx 4000\ \text{cm}^{-1}$. As a result, our theory is in a better agreement with the data after including the absorption of the pump beam; see Fig. 3. Using $p_{T,a} \approx 13.4$ nW for $p_{p,a} \approx 50$ mW, $L \approx 0.7\ \mu$m, $\tau_p \approx 180$ fs, $a_p \approx 0.126\ \text{mm}^2$, $n_p \approx n_{pg} \approx 3$, and $\alpha \approx 4000\ \text{cm}^{-1}$, we have estimated d_{eff} to be 5.31 nm/V by using Eq. (2). This value is 3 orders of magnitude higher than the nonresonant value [15]. Such a large difference could originate from resonance enhancement of the optical rectification. Above the bandgap of the InN films, the energy levels for the electrons and holes form a continuum that contributes to the resonance enhancement of the second-order nonlinear susceptibility. Indeed, such an enhancement was previously observed in a GaAs crystal [16]. As in [16], the photogenerated carriers in the InN films may also enhance the effective nonlinear coefficient. Based on our measurement made on each sample, we have determined the normalized conversion efficiency at the average pump power of 1 W. Among all samples studied by us, the highest value of the normalized conversion efficiency is $\tilde{\eta} \approx 360\ \text{mm}^{-2}$ for sample 7. This resonant value is 4 orders of magnitude higher than that for a ZnTe crystal.

In conclusion, we have investigated the resonant THz generation in InN films by using subpicoseconds laser pulses at 790 nm. Based on our experimental results it appears to us that optical rectification is one of the most plausible mechanisms for the THz generation in the InN films. The highest average output power generated by us is 0.931 μW. Such a relatively high power could be the manifestation of resonance enhancement. Additional work is necessary for us to fully understand the mechanism for the THz generation.

This work has been supported by the U.S. Air Force Office of Scientific Research and Air Force Research Laboratory.

References

1. G. L. Dakovski, B. Kubera, and J. Shan, J. Opt. Soc. Am. B **22**, 1667 (2005).
2. H. Liu, J. Xu, T. Yuan, and X.-C. Zhang, Phys. Rev. B **73**, 155330 (2006).
3. R. Ascázubi, I. Wilke, K. Denniston, H. Lu, and W. J. Schaff, Appl. Phys. Lett. **84**, 4810 (2004).
4. G. D. Chern, E. D. Readinger, H. Shen, M. Wraback, C. S. Gallinat, G. Koblmüller, and J. S. Speck, Appl. Phys. Lett. **89**, 141115 (2006).
5. K. A. Wang, Y. Cao, J. Simon, J. Zhang, A. Mintairov, J. Merz, D. Hall, T. Kosel, and D. Jena, Appl. Phys. Lett. **89**, 162110 (2006).
6. P. G. Huggard, C. J. Shaw, J. A. Cluff, and S. R. Andrews, Appl. Phys. Lett. **72**, 2069 (1998).
7. V. Y. Davydov, A. A. Klochikhin, R. P. Seisyan, V. V. Emtsev, S. V. Ivanov, F. Bechstedt, J. Furthmüller, H. Harima, A. V. Mudryi, J. Aderhold, and J. Graul, Phys. Status Solidi B **229**, R1 (2002).
8. J. Wu, W. Walukiewicz, W. Shan, K. M. Yu, J. W. Ager III, S. X. Li, E. E. Haller, H. Lu, and W. J. Schaff, J. Appl. Phys. **74**, 4457 (2003).
9. A. Yariv, *Quantum Electronics*, 3rd ed. (Wiley, 1989).
10. B. F. Levine, Phys. Rev. **7**, 2600 (1973).
11. F. N. H. Robinson, Phys. Lett. A **26**, 435 (1968).
12. X.-C. Zhang, B. B. Hu, J. T. Darrow, and D. H. Auston, Appl. Phys. Lett. **56**, 1011 (1990).
13. A. Zubrilov, in *Properties of Advanced Semiconductor Materials GaN, AlN, InN, BN, SiC, SiGe*, M. E. Levinshtein, S. L. Rumyantsev, and M. S. Shur, eds. (Wiley, 2001), pp. 49–66.
14. Y. J. Ding, IEEE J. Sel. Top. Quantum Electron. **10**, 1171 (2004).
15. V. I. Gavrilenko and R. Q. Wu, Phys. Rev. B **61**, 2632 (2000).
16. X.-C. Zhang, Y. Jin, K. Yang, and L. J. Schowalter, Phys. Rev. Lett. **69**, 2303 (1992).